JCTC Journal of Chemical Theory and Computation

Ab Initio Molecular Dynamics Study of a Highly Concentrated LiCl Aqueous Solution

L. Petit,[†] R. Vuilleumier,*[,‡] P. Maldivi,[†] and C. Adamo[§]

Laboratoire de Reconnaissance Ionique et de Chimie de Coordination, CEA - INAC/LCIB (UMRE 3 CEA-UJF), 17 rue des Martyrs, F-38054 Grenoble Cedex 9, France, Laboratoire de Physique Théorique de la Matiere Condensée, UMR7600, Université Pierre et Marie Curie, Paris, Tour 24 Boite 121, 4 place Jussieu, F-75252 Paris CEDEX 05, France, and Laboratoire d'Electrochimie et de Chimie Analytique, CNRS UMR-7575, Ecole Nationale Supérieure de Chimie de Paris, 11 rue P. et M. Curie, F-75231 Paris Cedex 05, France

Received January 5, 2008

Abstract: The properties of a highly concentrated aqueous lithium chloride solution (|LiCl| = 14 mol L^{-1}) are investigated using Car−Parrinello molecular dynamics. The coordination spheres of lithium ions, chloride ions, and water molecules are described successively. On the whole, our simulation provides results—distances and coordination numbers—in very good agreement with experimental data. The lithium solvation shell is found to exhibit a tetrahedral configuration on average, with three stable clusters observed during the simulation: Li^+-4H_2O, $Li^+(H_2O)_3Cl^-$, and $Li^+(H_2O)_2(Cl^-)_2$. The chloride coordination sphere is logically formed by strong Cl−H hydrogen bonds with neighboring water molecules, for a mean coordination number of 4.4. The structuring of water molecules is strongly affected by the high concentration in LiCl. The hydrogen bond network is globally broken down, but little variation is calculated on water dipoles (μ = 3.07 D) because of the strong polarization from Li^+ and Cl^- ions. We also point out some of the characteristic features of such a highly concentrated solution: water bridging between Li^+ and Cl^- hydration spheres, Li^+-Cl^- ion-pairing, and intermediate behavior between dilute solutions and molten salts. Finally, the reliability of our simulation to describe ion-pairing is discussed.

1. Introduction

Lithium chloride aqueous solutions have been extensively studied because of their implication in many fields: biology, medicine, or electrochemistry. LiCl also dissolves outstandingly well in water because of the strong difference in the ionic radius between lithium and chloride ions,[1,2] making them suitable prototypes to investigate the properties of ionic complexes in highly concentrated aqueous solutions. To date, there has been considerable experimental work on the properties of LiCl solutions, with various methods: viscosimetry measurements,[3,4] NMR and Raman spectroscopies,[5,6] X-ray diffraction,[7−10] and especially neutron diffraction.[9,11−21] Yet, the isotopic substitution technique used to analyze neutron diffraction patterns[22,23] has been several times called into question because of large statistical errors.[17,23] More generally, all of these methods do not provide access to the detailed microscopic structure of LiCl, and the structuring of water surrounding the ions is usually clouded by the bulk water response. Theoretical methods, based on QM/MM,[24,25] Monte Carlo,[26,27] classical molecular dynamics approaches,[2,28−31] have been proposed to overcome such limitations, successfully or not. For instance, classical molecular dynamics seem to be dramatically dependent on the type of model used to describe the atomic interactions and, in particular, whether polarizability effects are considered. Egorov et al.[28] have compared the results from three different interaction potentials on LiCl solutions over a wide range of concentrations.

* Corresponding author e-mail: vuilleum@lptl.jussieu.fr.
[†] Laboratoire de Reconnaissance Ionique et de Chimie de Coordination.
[‡] Université Pierre et Marie Curie.
[§] Ecole Nationale Supérieure de Chimie de Paris.

10.1021/ct800007v CCC: $40.75
Published on Web 05/30/2008

They found that the structure of the Li^+-H_2O interaction is indeed strongly dependent on the potential, with coordination numbers ranging from 4 to 6.

For a few years now, first principles molecular dynamics have been carried out to study ion solvation in water at low concentrations, and results are globally in very good agreement with experimental data.[32–44] They provide a fine description of the microstructure of both the solute and solvent and should thus enable the treatment of LiCl solutions in a more unbiased way than classical molecular dynamics. These simulations pave the way for the study of electrolyte solutions at higher concentrations as well as the study of solvation effects of metal ions in electrolyte solutions.

For instance, highly concentrated solutions of lithium chloride have been used to model the complexation of chloride ions to trivalent f elements,[45] complexes that are assumed to be formed in geological salt formations when nuclear wastes are being stored. Yet, the coordination sphere of f elements in LiCl aqueous solutions is still uncertain (see ref 46 and references therein for more details), and theoretical studies could thus help to clarify this aspect. In the following, we study the local structure of a highly concentrated lithium chloride solution (|LiCl| = 14 M) with Car−Parrinello molecular dynamics[47] based on density functional theory (DFT). Previous works have demonstrated the ability of DFT to describe the solvation of Li^+ and Cl^- ions at infinite dilution.[34–36,41,43,48] Yet, to our knowledge, such a technique has never been applied to LiCl aqueous solutions. Our ultimate goal is to use ab initio molecular dynamics to investigate the coordination sphere of trivalent f elements in such a solution. The present work must thus be considered as a preliminary step to check the reliability of our calculations as well as a way to solve some of the uncertainties that still remain about the local structure of LiCl solutions at high concentrations.

2. Computational Details

The simulation was performed with the CPMD code.[49] The BP86 GGA functional[50] was applied throughout as this functional has already proved to provide a reliable description of f elements complexes,[51,52] while it leads to a reasonable description of pure water.[53] We have thus kept this functional in order to ensure a consistent study with the next work including f elements (see the Introduction). Troullier−Martins norm-conserving pseudopotentials[54] were used along with the Kleinman−Bylander decomposition for all Li, Cl, O, and H atoms.[55] The reference electronic configurations for O, H, and Cl were the neutral atoms. Pseudization radii of s = p = 1.52 au for chlorine, 2s = 2p = 3d = 1.05 au for oxygen, and 1s = 2p = 0.5 au for hydrogen atoms were used. The pseudopotentials for BP are similar to those used in ref 36 for the simulation of Cl^- in liquid water, where they were shown to correctly describe the chloride−water interaction. For lithium, we have employed a semicore pseudopotential starting from Li^+ as a reference configuration. The pseudization radius of the 1s electrons was set to 0.51 au. In the CPMD simulation, the electronic wave functions have been expanded in a plane-waves basis set up to the energy cutoff of 70 Ry. Pseudopotentials and the cutoff were checked on $Cl^-−H_2O$ and $Li^+−H_2O$ systems by comparing the CPMD optimized structures and interaction energies with that obtained from Gaussian 03 (MP2 and BP86, 6-311++G(d,p); ref 56). Discrepancies are very low between CPMD and G03/BP86 calculations, and they do not exceed 0.09 Å on distances and 1.5 kcal/mol on energies with respect to MP2 results (see Table 1).

Table 1. Comparison of Geometries and Interaction Energies (E_{int}) between Gaussian 03 (DFT or MP2) and CPMD (BP86, Trouiller−Martins Pseudopotentials) Calculations[a]

	G03/MP2/ 6-311++G(d,p)	G03/BP86/ 6-311++G(d,p)	CPMD/ BP86
	$Li^+−H_2O$		
d(Li−O), Å	1.86	1.86	1.86
d(O−H), Å	0.96;0.96	0.97;0.97	0.98;0.98
($\hat{LiOH}$), deg	127.6;127.6	127.4;127.4	126.7;128.3
E_{int}, kcal/mol	−33.4	−32.5	−32.4
	$Cl^-−H_2O$		
d(Cl−H), Å	2.15	2.10	2.06
d(O−H), Å	0.98;0.96	1.01;0.97	1.02;0.97
($\hat{HOCl}$), deg	165.4	168.8	174.1
E_{int}, kcal/mol	−13.7	−15.2	−15.2

[a] Gaussian interaction energies are BSSE-corrected.

A preliminary classical molecular dynamics step was performed with the Moldy package[57] to get a reliable initial configuration for the CPMD simulation as well as to determine an adequate size for the periodic box. The Lennard-Jones 12-6 potential was taken from Dang[58] following the previous simulations by Egorov et al.[28] Simulations were carried out for 400 ps on three different sizes of box with a density of 1.196 corresponding to a concentration of 14 M (box 1, 243 H_2O, 50 LiCl; box 2, 60 H_2O, 12 LiCl; box 3, 30 H_2O, 6 LiCl). The system containing 30 H_2O, 6 Cl^-, and 6 Li^+ was found to give reasonable results compared to larger boxes and was thus kept for the CPMD simulation.

The Car−Parrinello simulation was performed in a cubic box of size 10.33 Å with periodic boundary conditions. To ensure an accurate description of structural properties, we have taken the fictitious mass μ = 200 au, while the time step was set to 3.0 au (0.072 fs). This choice should allow for negligible dependency of our results with respect to the unphysical parameter μ.[59] The temperature was first fixed to 300 K for 5 ps to make the system equilibrate, and then the trajectories were sampled for 25 ps in the NVE ensemble. To compute molecular dipole moments, the maximally localized Wannier functions[60] were collected every 10 steps for the first 15 ps of the simuation.

In the following, the program VMD[61] was used for visualizations. Radial distribution functions $g(r)$ were also analyzed with VMD. Corresponding $g(r)$ results are presented from 0 to 5 Å to avoid double-counting due to periodic boundary conditions.

3. Results and Discussion

3.1. Lithium Ions Coordination Sphere. The radial distribution functions of lithium ions are depicted in Figure

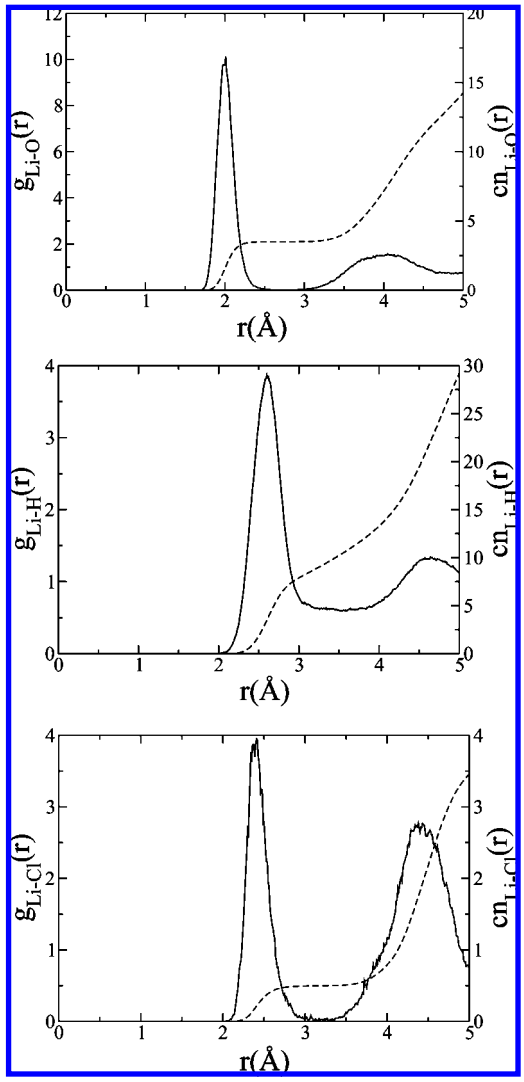

Figure 1. Radial distribution function *g* (full line) and coordination number cn (dashed line) for the Li^+-O, Li^+-H, and Li^+-Cl^- interactions.

1, while the first peaks are detailed in Table 2. We first focus on the interaction between Li^+ and water molecules. The first Li−O peak at 2.01 Å compares nicely with the experimental values determined by neutron diffraction. This first peak is quite sharp. It is followed by a well-defined minimum, which indicates that the lithium first hydration sphere is fairly rigid and clearly separated from the second one. This may be the result of the small size and high electronegativity of the Li^+ ion, which makes the Li−O interaction quite strong and thus prevents the exchange of water molecules with outer hydration spheres. Actually, comparisons with studies at lower concentrations in LiCl show that the Li−O distance is rather constant, whereas the coordination number is much more dependent on concentration.[17] From the integration of the first peak of $g(r)$, we found 3.5 water molecules on average around each lithium ion (Table 2). Such a value does not mean that the lithium coordination sphere is mobile but comes from a balance between three stable clusters: Li^+-4H_2O, $Li^+(H_2O)_3Cl^-$, and $Li^+(H_2O)_2(Cl^-)_2$. There are indeed several occurences of Li^+-Cl^- ion pairing, as will be discussed in section 3.5. For all three clusters, the total coordination number of Li^+ ions is 4. Actually, we observe four Li^+-4H_2O clusters, one $Li^+(H_2O)_3Cl^-$ cluster, and one $Li^+(H_2O)_2(Cl^-)_2$ cluster, leading to the calculated Li−O coordination number of 3.5. Such a value is in agreement with experimental data, but longer and probably larger simulations are needed to provide a definitive picture (see also the discussion in section 3.5). Snapshots illustrating these three clusters are displayed in Figure 2. The oxygen atoms of the water molecules and the chloride ions occupy the vertices of a slightly distorted tetrahedron. The angular distribution (O−*Lî*−O) is centered at 108.6° and shows that a tetrahedral-like configuration (109°) is indeed found.

The impact of the lithium ion on the second coordination sphere is much less pronounced. As can be seen from Figure 1, the second peak of g_{LiO} is located around 4 Å but is rather flat and not well-resolved. It also partially penetrates into the following peak, suggesting an exchange between the water molecules of the second hydration shell and the bulk. The agreement with the experimental value (4.4−4.7 Å; ref 7) becomes poorer, but this is the only experimental result we have found describing the second solvation shell. Note that the concentration in this work is lower than ours (10 M).

Even so, the second peak shows evidence of the structuring of the lithium second coordination sphere, as sketched in Figure 3. The Li−O distance is 2.0 Å, while, as will be shown in section 3.3, the O−O distance is around 2.8 Å (Table 2). If the solution was totally unstructured, we should observe the second peak for the Li−O interaction around 4.8 Å. In our simulation, this distance is reduced to 4.0 Å. From Figure 3, it is then clear that the (Li−*Ô*−O) angle is near 109°, that is, close to a tetrahedral configuration around oxygen atoms of the first solvation shell.

3.2. Chloride Ions Coordination Sphere. As for the lithium coordination sphere, we give in Figure 4 the radial distribution functions for the Cl^- ion, while more details on the main peaks can be found in Table 3. The positively charged hydrogen atoms of the water molecules are oriented toward the negatively charged chloride ions, forming hydrogen bonds. The first peak is thus due to the Cl−H interaction and is calculated at 2.13 Å. It is well-defined, but the nonzero minimum of the radial distribution function indicates that the water molecules in the first coordination sphere are more mobile than with the lithium ion. Integration yields to a coordination number of 4.4 hydrogen atoms around each chloride ion, but this is not straightforward to interpret. Indeed, because of ion pairing, the radial distribution function of Cl−O interaction takes into account water molecules that belong to the lithium first coordination sphere. This could explain how we can find more oxygen atoms (5.7) than hydrogen atoms (4.4) around each chloride ion.

The second Cl−H peak is not sharply defined, lying around 3.6 Å. In Figure 4, we observe that it is actually divided into two lower peaks, showing that the different hydration shells can interpenetrate each other.

Even though the chloride first hydration sphere is found to be rather flexible, hydrogen bonds should be nevertheless quite strong, as it is well-known that hydrogen bonds involving charged ions feature high binding energies. This

Table 2. Structural Parameters for the Li^+ Hydration[a]

	CPMD calc.		experiment				
	r, Å	cn	*r*, Å	cn	|LiCl|	technique	ref
Li−O, 1st peak	2.01	3.5	1.95 ± 0.02	3.3 ± 0.5	9.95 m	ND	15
			1.96 ± 0.02	3.2 ± 0.2	14 m	ND	17
			2.01 ± 0.05	4 ± 1	9.5 m	ND	19
			2.22 ± 0.02	4	13.75 M	ND	9
			1.95 ± 0.02	3.3 ± 0.5	9.95 m	ND	20
Li−O, 2nd peak	≃4.0		4.4−4.7		10 M	XRD	7
			4.5		9.95 m	ND	15
Li−H, 1st peak	2.60	≃8.7	2.50 ± 0.2		9.95 m	ND	15
			2.52 ± 0.02		14 m	ND	17
			2.61 ± 0.05		9.5 m	ND	19
			2.68 ± 0.01		13.75 M	ND	9
			2.50 ± 0.02		9.95 m	ND	20
Li−Cl, 1st peak	2.41	0.5	2.76	1.5	12.8 m	ND	74
Li−Cl, 2nd peak	4.38		3.28	7.4	12.8 m	ND	74

[a] *r* is the interatomic distance, and cn is the coordination number. ND, neutron diffraction; XRD, X-ray diffraction. M = mol L^{-1}; m = mol kg^{-1}.

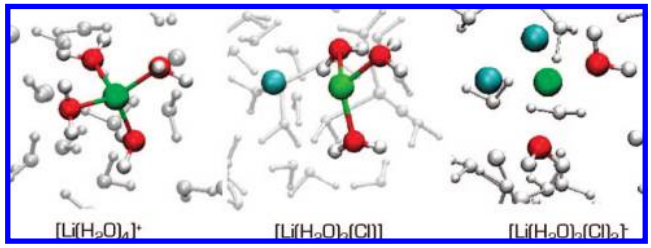

Figure 2. Representation of the three stable clusters for the lithium coordination sphere. Lithium is in green, chloride in blue, oxygen in red, and hydrogen in white.

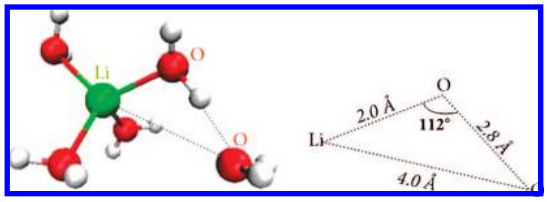

Figure 3. Sketch of the interaction between one lithium ion and two water molecules.

can be assessed through intermolecular distances, as shorter interatomic distances correspond to stronger hydrogen bonds.[62] In our simulation, the Cl−H distance (2.13 Å) is clearly shorter than the sum of the Cl^- and H radii (r_{Cl^-} = 1.81 Å, r_H = 0.53 Å), and Cl−H hydrogen bonds must thus be rather strong and stable. As given in Table 3, the first oxygen atoms are found at 3.13 Å, which exactly corresponds to the sum of the Cl−H distance (2.13 Å) and the O−H distances (1.01 Å). This indicates that the Cl−H_2O interaction is quite directional with $(Cl-\hat{H}-O) \simeq 180°$. Such an intermediate position of the hydrogen atom along the connecting line between Cl and O atoms is also very favorable for the hydrogen bond strength.[63]

To get further insights into chloride ions' behavior, the g_{Cl-Cl} radial distribution function is also plotted in Figure 4. In agreement with neutron diffraction patterns,[11,64] there are two dominant peaks. They are badly resolved because the total number of chloride ions in the simulation box is too low, and the statistics are thus rather inaccurate. The first peak is calculated at 3.81 Å, versus 3.75 Å and 4.2 Å for the experimental counterparts. In our simulation as well as

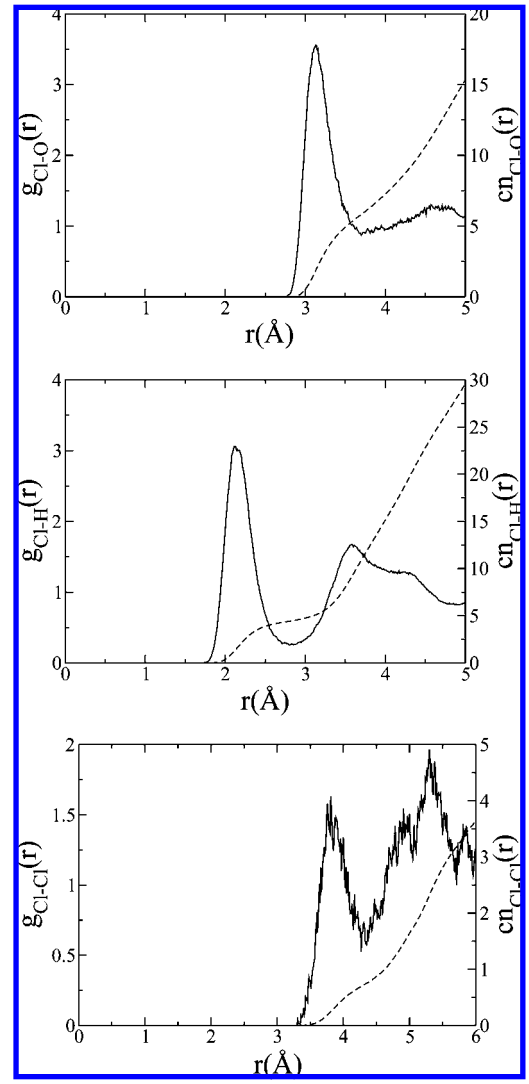

Figure 4. Radial distribution functions *g* (full line) and coordination number cn (dashed line) for the Cl^-−O, Cl^-−H, and Cl^-−Cl^- interactions.

in experimental measurements, this peak is assigned to the interaction between the chloride ions involved in ion pairing. It is actually quite characteristic of LiCl molten salts, for which it is indeed attributed to Li^+−Cl^- direct contact.[11]

Table 3. Structural Parameters for the Cl^- Hydration[a]

	CPMD calc.		experiment				
	r, Å	cn	*r*, Å	cn	|LiCl|	method	ref
Cl−O, 1st peak	3.13	5.7	3.10		11 M	XRD	10
			3.29 ± 0.04	5.3 ± 0.2	9.95 m	ND	14
Cl−H, 1st peak	2.13	4.4	2.22 ± 0.02		9.95 m	ND	14
			2.24	4.4 ± 0.3	14.9 m	ND	11
			2.225		9.2 M	ND	18
			2.238 ± 0.006		13.75 M	ND	9
Cl−H, 2nd peak	3.59		3.5−3.7		9.95 m	ND	14
			3.56 ± 0.04		14.9 m	ND	11
			3.625		9.2 M	ND	18
Cl−Cl, 1st peak	3.81	≃0.7	3.75 ± 0.03	2.3 ± 0.3	14.9 m	ND	11
			4.2 ± 0.1	1.2 ± 0.5	8.6 m	ND	64
Cl−Cl, 2nd peak	5.3		6.38 ± 0.03	10.0 ± 0.5	14.9 m	ND	11
			6.4 ± 0.2	7.0 ± 1.0	8.6 m	ND	64

[a] *r* is the interatomic distance, and cn is the coordination number. ND, neutron diffraction; XRD, X-ray diffraction. M = mol L^{-1}; m = mol kg^{-1}.

Table 4. Structural Parameters for the Water Molecules[a]

	CPMD, calcd		experiment, LiCl					experiment, pure water		
	r, Å	cn	*r*, Å	cn	|LiCl|	method	ref	*r*, Å	cn	ref
O−H, 1st peak, intra	1.01	2.0	0.97 ± 0.02		10 m	ND	12	1.02 ± 0.02		76
			0.97		9.2 M	ND	18	0.966 ± 0.006		77
			0.970 ± 0.002		13.75 M	ND	16			
			0.940 ± 0.005		13.75 M	ND	9			
O−H, 2nd peak, H-bond	1.71	3.0 (1.0)	1.8 ± 0.1		10 m	ND	12	1.87 ± 0.04		76
O−H, 3rd peak, inter	3.20		3.5 ± 0.4		10 m	ND	12	3.3 ± 0.2		76
H−H, 1st peak, intra	1.60	1.0	1.55 ± 0.02		10 m	ND	12	1.50 ± 0.02	1.2 ± 0.1	76
			1.57		9.2 M	ND	18	1.51 ± 0.03		77
			1.59 ± 0.01		13.75 M	ND	16			
			1.487 ± 0.006		13.75 M	ND	9			
H−H, 2nd peak, H-bond	2.26	3.8 (2.8)	2.3 ± 0.06		10 m	ND	12	2.44 ± 0.04	6.0 ± 0.4	76
H−H, 3rd peak, inter	≃3.65		3.8 ± 0.2		10 m	ND	12	3.8 ± 0.2	30 ± 4	76
O−O, 1st peak, H-bond	2.71	3.0	2.85		13.75 M	ND	9			
O−O, 2nd peak, inter	3.26	5.3 (2.3)						3.6	5.2 ± 0.04	78
O−O, 3rd peak, inter	≃4.25							4.5		78

[a] *r* is the interatomic distance, and cn is the coordination number. Coordination numbers in parentheses correspond to the real integration; i.e., they take into account previous peaks. ND, neutron diffraction. M = mol L^{-1}; m = mol kg^{-1}.

Degreve and Mazzé[2] have noticed that a Cl−Cl distance around 3.8 Å is close to the sum of the ionic radii of two chlorides (r_{Cl^-} =1.81 Å) and that such a short distance between two anions is only possible if a cation is close enough to provide electrostatic stabilization. This is particularly the case for the observed $Li^+(H_2O)_2(Cl^-)_2$ cluster, although a coordination number around 0.7 indicates that this is not the only occurrence of Cl−Cl close contact. In contrast, the second peak found in the interval from 4.5 to 5.7 Å (as explained in the Computational Details, the radial distribution function is strictly valid only between 0 and 5 Å, so the reliability of the second peak at 5.3 Å is questionable), with a maximum at 5.3 Å, is consistent with the usual distance between two solvated chloride ions at a lower dilution. This has already been suggested by Neilson and Enderby[65] for a dilute solution of $NiCl_2$. It is interesting to compare these two peaks, as they underline the intermediate character of our concentrated LiCl solution (14 M) between a dilute solution (2nd peak) and a molten salt (1st peak). The first peak, experimentally observed, is a signature of Li−Cl ion pairing in highly concentrated LiCl solutions.

3.3. Water Structure. Distances and coordination numbers for water molecules in concentrated lithium chloride (14 M) are listed in Table 4. Radial distribution functions for the O−H and O−O interactions are also displayed in Figure 5. They are compared to available experimental results for LiCl solutions at close concentration. In the last columns, data for pure liquid water are also presented for comparison. In order to make the analysis easier, the main peaks are classified according to their nature: intramolecular ("intra"), intermolecular ("inter"), or hydrogen-bonding ("H-bond") interactions.

In Table 4, the peak centered at 1.01 Å is logically associated with the intramolecular O−H bond, in agreement with experimental values. As observed by Jal et al.[18] with neutron diffraction, no discrepancy is found in the intramolecular water structure with respect to pure water. There is in contrast a small increase in the H−H intramolecular distance with respect to pure water, but there is no straightforward link with the interaction with Li^+ and Cl^- ions. In particular, the angular distribution (H−$\hat{O}$−H) is centered at 104.4° and remains close to the value in pure water (104.5°, ref 66).

As could be expected, the hydrogen-bonding network is more affected. We globally observe a strong reorganization of the bulk solvent with respect to dilute solutions. In pure water, molecules are usually arranged in a tetrahedral network: each oxygen atom accepts two hydrogen bonds

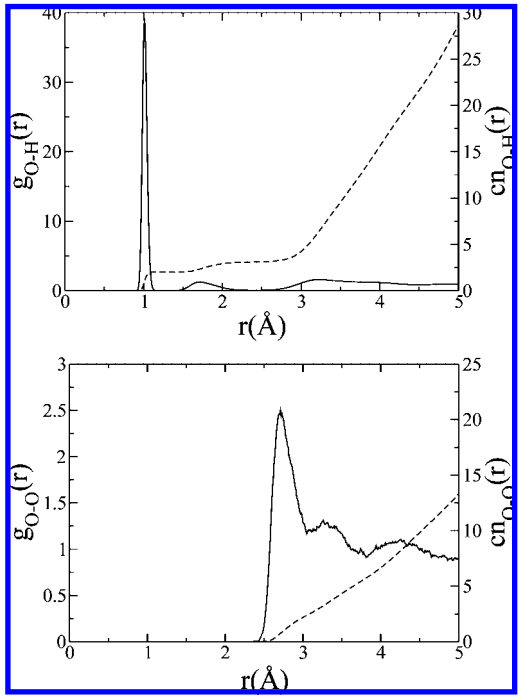

Figure 5. Radial distribution functions *g* (full line) and coordination number cn (dashed line) for the O−H and O−O interactions.

from neighboring water molecules, and nearly every hydrogen atom interacts with another oxygen atom. In our simulation, oxygen atoms accept only one hydrogen bond on average, as the H-bond peak of g_{OH} integrates for 1.0. Disruption of the water structure is further suggested by the mixing of g_{HH} peaks at a high LiCl concentration, which are normally well-defined at 2.44 and 3.8 Å in pure water. The length of O···H hydrogen bonds is more difficult to understand. We can indeed expect from the general breakdown of the solvent structuring that hydrogen bonds should be weakened in our solution with respect to pure water, and so their length should increase. In Table 4, we observe the opposite trend: the O−H hydrogen bonds goes from 1.87 Å in pure water to 1.71 Å in our calculations. This shortening may be overestimated in our simulation, but the global trend is actually correct, as can be seen from the available experimental data on LiCl solutions (1.8 Å, see Table 4). We think this could be the result of a positive cooperation effect between ions and water molecules. Oxygen atoms interacting with lithium ions are strongly polarized; their hydrogen atoms become more acidic, and thus hydrogen bonds can be locally strengthened.

Finally, because of the high concentration in LiCl, there is a deficiency in water molecules in our solution. Lithium and chloride ions must then share their coordination sphere, and indeed we observe several occurrences of water-bridging configurations in our simulation. Figure 6 shows how they arrange one another, the negatively charged oxygen atoms interacting with the cation Li^+, while the positive hydrogen atoms are oriented toward chlorides. No bifurcated hydrogen bond, that is, one chloride anion forms two hydrogen bonds with the two hydrogen atoms of a water molecule, is nevertheless observed during the simulation.

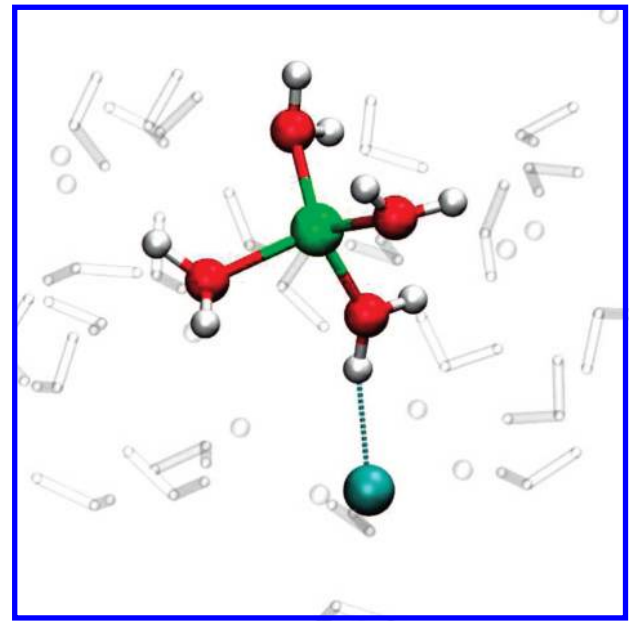

Figure 6. Water bridging between Li^+ and Cl^- ions: lithium in green, chloride in blue, oxygen in red, and hydrogen in white.

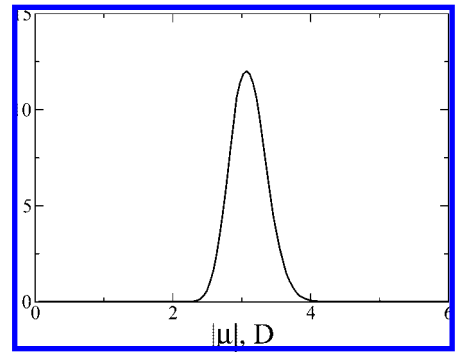

Figure 7. Distribution of the dipole moment of water molecules in |LiCl| = 14 M.

3.4. Dipole Moments. In order to assess these effects on the electronic structure of water molecules, we have estimated their dipole moments. The molecular charge distribution was studied using maximally localized Wannier functions. These provide an unambiguous way to assign dipole moments to molecules. The dipole moment of water molecules in pure water has been previously estimated with Car−Parrinello molecular dynamics as being on the order of 3.0 D by Silvestrelli and Parrinello.[2,68] This value is very close to the value proposed by Badyal et al.,[69] 2.9 ± 0.6 D, for pure water, from an analysis of the experimental X-ray diffraction form-factor. Other theoretical values were also proposed; see, for instance, refs 68− 72. The dipole moment distribution found in our simulation features a main peak at 3.07 D (Figure 7). We thus do not find a strong influence of the electrolytes on the dipole moment of water molecules. The effect of broken hydrogen bonds is compensated by the strengthening of the remaining bonds and polarization by the Li^+ and Cl^- ions.

3.5. Discussion. In order to rationalize the structuring of water in electrolyte solutions, Collins[1] has proposed a general principle in which ions are classified as being either structure-

maker or structure-breaker ions. Structure-maker ions bind tightly to water molecules and thus form well-defined ion−water complexes. In contrast, structure-breaker ions give weak interactions with water molecules, and their hydration sphere is thus quite mobile. The lithium ion is small, with a high charge density, and is thus classified as a structure-maker ion. Its interaction with surrounding water molecules is quite strong, and its hydration sphere is oriented so as to give favorable electrostatic interactions.[73] Chlorides are usually considered to be structure-breaker ions because of their fairly large ionic radii, and their hydration sphere is thus much more flexible than for lithium. Hribar et al.[73] have shown with Monte Carlo simulations that the organization of water molecules results from a balance between two competitive effects: the ion−water interaction, which is governed by electrostatic effects (charge densities), and water−water interactions that are stabilized by hydrogen bonding. They confirmed that, for small cations like Li^+, the high charge density favors strong electrostatic interactions with nearby water molecules, but such a strong ordering of water molecules also decreases their ability to form a well-structured hydrogen-bond network. This is indeed what we observe in the present simulation.

According to Collins' classification also,[1] ion pairing mainly occurs between similarly sized ions that belong to the same category, either structure-maker or structure-breaker. Thus, lithium and chloride ions should have a low tendency to get in direct contact, and they best remain apart in solution, explaining their high solubility in water. Even so, there has been a long debate about the occurrence of ion pairing between Li^+ and Cl^- ions for highly concentrated solutions.

A very recent simulation with the reverse Monte Carlo method has shown that there was no chloride ion within the lithium first coordination sphere, even at saturation.[27] Yet, most neutron diffraction works,[11,17,64,74] many of them quite recent, have evidenced ion pairing for concentrated solutions, either directly through the Li^+-Cl^- radial distribution function or indirectly with the Cl^-Cl^- interaction around 3.8 Å, as discussed in section 3.1.[11,64] Rudolph et al.[6] have studied, with Raman spectroscopy, aqueous LiCl solutions from saturation to low concentration. They also showed that ion pairing occurs at high concentrations through the Li−Cl vibration around 376 cm^{-1}, which was not observed for a more dilute solution. X-ray Compton scattering experiments[75] as well as molecular dynamics simulations[2,30] also support the existence of ion pairing.

In our simulation, there is clear evidence that chloride can enter the lithium first coordination sphere, as we find the Li−Cl mean distance to be 2.41 Å, versus 2.01 Å for the first oxygen atoms and 2.60 Å for hydrogen atoms (see Table 2). This peak is badly resolved but is quite thin and integrates for 0.5 chloride on average (see Figure 1). Only one piece of experimental data is available for this distance, from Ichikawa et al.,[74] and exhibits a Li^+-Cl^- direct contact around 2.76 Å. Degreve and Mazzé[2] have obtained from molecular dynamics a distance of 2.20 Å. With increasing LiCl concentration, the number of water molecules available to interact with the lithium ion becomes smaller, and at

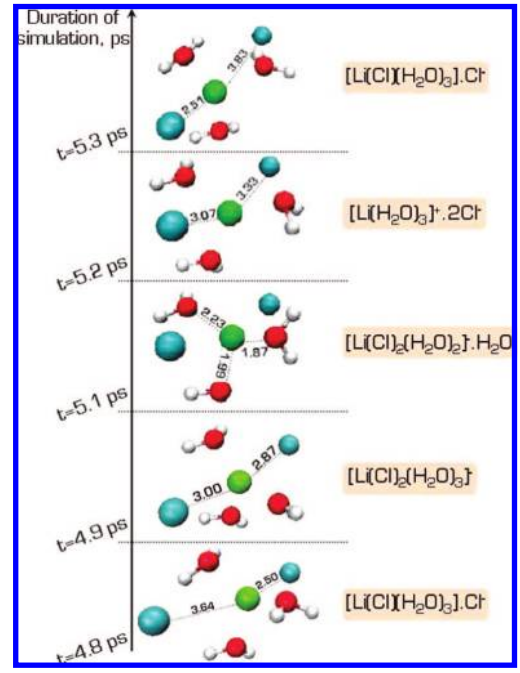

Figure 8. Exchange of chloride ions in lithium first coordination sphere. Distances are given in angtröms. Lithium is in green, chlorides are in blue, oxygen atoms in red, and hydrogen atoms in white.

14 M, there are not enough water molecules left to complete the lithium cation coordination sphere. Chlorides can then penetrate the lithium hydration shell to form ion pairs, as represented in Figure 2.

In the Computational Details, we have specified that the starting configuration for the ab initio MD simulation is based on a classical molecular dynamics calculation performed with the Lennard-Jones potential, as proposed by Dang.[58] This preliminary step already predicts direct contact between Li^+ and Cl^- ions, and we logically wondered if this initial configuration could have biased our results. Indeed, the concentration in our simulation is so high that atoms could hardly be displaced from their position at the end of the classical MD step. We have thus compared the Li^+-Cl^- radial distribution function patterns in our simulation with that obtained by Egorov et al.[28] from the Dang potential with classical MD for the Li−Cl interaction. Results are rather close since both plots show a quite pronounced first peak around 2.4 Å, followed by a smoother peak between 4 and 5 Å. The residence time of water molecules around lithium ions is usually assessed in the range 30−100 ps,[30,31] so no full reorganization of water in the lithium coordination sphere is expected from an ab initio simulation. In contrast, the Li^+-Cl^- interaction has been calculated to be much shorter, on the order of 4.5 ps, and our simulation should thus be long enough (30 ps total) to allow the breakdown of ion pairing. And indeed, we do observe chloride exchange in the lithium first coordination sphere during our simulation. In Figure 8, we have represented how one of these exchanges occurs: starting at the end of the thermalization (4.9 ps), one chloride ion enters a lithium coordination sphere. There are then five neighbors around the lithium ion ($2Cl^- + 3H_2O$), whereas the common coordination number is 4. Because of

the steric hindrance, two transient configurations are then observed: in the first one, at 5.1 ps, one water molecule tends to move away from the cation (d(Li−O) = 2.23 Å), while in the next configuration (t = 5.2 ps), both chloride ions are pulled away. Only one chloride finally moves to the second coordination sphere, and the initial coordination shell is restored. It is also of importance to underline that the mean square displacement of chloride ions and oxygens atoms is about 1.5 Å^2. This indicates that limited rearrangement occurs but that Cl and O atoms do move away from their initial coordination cage. This is further confirmed by the strong modification in distances with respect to the classical MD results. Of course, a longer simulation could provide a more clear-cut vision of ion pairing and of the related number of water molecules in the solvation shell of Li^+. Starting from another initial configuration could also be a relevant way to check our results. Even so, as most experimental data, our simulation agrees with the occurrence of ion pairing.

4. Conclusion

We have studied, with ab initio molecular dynamics, the local structure and behavior of a highly concentrated aqueous solution of lithium chloride. The structure of the ion hydration spheres is very well reproduced, with a long-lived tetrahedral configuration for the lithium ion, and six water molecules around chloride anions. The water structure is deeply affected for such a high concentration: hydrogen bonds are massively disrupted, and there is also evidence of water-bridging configurations between Li^+ and Cl^- hydration spheres because of the low content in water molecules. Few occurrences of ion pairing have also been observed, showing the intermediate character between solution and ionic liquid. Interatomic distances are in very good agreement with both experimental and theoretical results, as are the observed coordination numbers. The latter, especially around Li^+, may be affected by the simulation length because of the long time scale of water exchange around Li^+. However, this is very encouraging for a future study on the coordination sphere of f elements in concentrated LiCl.

Acknowledgment. We would like to thank the Centre de Calcul Recherche et Technologie (CCRT) for a generous allocation of computer time.

References

(1) Collins, K. D. *Biophys. J.* **1997**, *72*, 65.

(2) Degreve, L.; Mazzé, F. M. *Mol. Phys.* **2003**, *101*, 1443.

(3) Martin, J. M.; Berntsson, T. S. *J. Chem. Eng. Data* **1994**, *39*, 68.

(4) Moynihan, C. T.; Balitactac, N.; Boone, L.; Litovitz, T. A. *J. Chem. Phys.* **1971**, *55*, 3013.

(5) Bryant, R. G. *J. Phys. Chem.* **1969**, *73*, 1153.

(6) Rudolph, W.; Brooker, M. H.; Pye, C. C. *J. Phys. Chem.* **1995**, *99*, 3793.

(7) Lawrence, R. M.; Kruh, R. F. *J. Chem. Phys.* **1967**, *47*, 4758.

(8) Brady, G. W. *J. Chem. Phys.* **1958**, *28*, 464.

(9) Narten, A. H.; Vaslow, F.; Levy, H. A. *J. Chem. Phys.* **1973**, *58*, 5017.

(10) Yamanaka, K.; Yamagami, M.; Takamuku, T.; Yamaguchi, T.; Wakita, H. *J. Phys. Chem.* **1993**, *97*, 10835.

(11) Copestake, A. P.; Neilson, G. W.; Enderby, J. E. *J. Phys. C: Solid State Phys.* **1985**, *18*, 4211.

(12) Tromp, R. H.; Neilson, G. W.; Soper, A. K. *J. Chem. Phys.* **1992**, *96*, 8460.

(13) Ohtomo, N.; Arakawa, K. *Bull. Chem. Soc. Jpn.* **1979**, *52*, 2755.

(14) Cummings, S.; Enderby, J. E.; Neilson, G. W.; Newsome, J. R.; Howe, R. A.; Howells, W. S.; Soper, A. K. *Nature* **1980**, *287*, 714.

(15) Newsome, J. R.; Neilson, G. W.; Enderby, J. E. *J. Phys. C: Solid State Phys.* **1980**, *13*, L923.

(16) Ichikawa, K.; Kameda, Y. *J. Phys.: Condens. Matter* **1989**, *1*, 257.

(17) Howell, I.; Neilson, G. W. *J. Phys.: Condens. Matter* **1996**, *8*, 4455.

(18) Jal, J. F.; Soper, A. K.; Carmona, P.; Dupuy, J. *J. Phys.: Condens. Matter* **1991**, *3*, 551.

(19) Yamagami, M.; Yamaguchi, T.; Wakita, H. *J. Chem. Phys.* **1994**, *100*, 3122.

(20) Enderby, J. E.; Neilson, G. W. *Rep. Prog. Phys.* **1981**, *44*, 38.

(21) Kameda, Y.; Suzuki, S.; Ebata, H.; Usuki, T.; Uemura, O. *Bull. Chem. Soc. Jpn.* **1997**, *70*, 47.

(22) Ohtaki, H.; Radnai, T. *Chem. Rev.* **1993**, *93*, 1157.

(23) Ansell, S.; Barnes, A. C.; Mason, P. E.; Neilson, G. W.; Ramos, S. *Biophys. Chem.* **2006**, *124*, 171.

(24) Tongraar, A.; Liedl, K. R.; Rode, B. M. *Chem. Phys. Lett.* **1998**, *286*, 56.

(25) Loeffler, H. H.; Mohammed, A. M.; Inada, Y.; Funahashi, S. *Chem. Phys. Lett.* **2003**, *379*, 452.

(26) Asada, T.; Nishimoto, K. *Chem. Phys. Lett.* **1995**, *232*, 518.

(27) Harsànyi, I.; Pusztai, L. *J. Chem. Phys.* **2005**, *122*, 124512.

(28) Egorov, A. V.; Komolkin, A. V.; Chizhik, V. I.; Lyubartsev, A. P.; Laaksonen, A. *J. Phys. Chem. B* **2003**, *107*, 3234.

(29) Hermansson, K.; Wojcik, M. *J. Phys. Chem. B* **1998**, *102*, 6089.

(30) Du, H.; Rasaiah, J. C.; Miller, J. D. *J. Phys. Chem. B* **2007**, *111*, 209.

(31) Impey, R. W.; Madden, P. A.; McDonald, I. R. *J. Phys. Chem.* **1983**, *87*, 5071.

(32) White, J. A.; Schwegler, E.; Galli, G.; Gygi, F. *J. Chem. Phys.* **2000**, *113*, 4688.

(33) Vuilleumier, R.; Sprik, M. *J. Chem. Phys.* **2001**, *115*, 3454.

(34) Lyubartsev, A. P.; Laasonen, K.; Laaksonen, A. *J. Chem. Phys.* **2001**, *114*, 3120.

(35) (a) Laasonen, K.; Klein, M. L. *J. Phys. Chem. A* **1997**, *101*, 98. (b) Laasonen, K.; Klein, M. L. *J. Am. Chem. Soc.* **1994**, *116*, 11620.

(36) Heuft, J. M.; Meijer, E. J. *J. Chem. Phys.* **2003**, *119*, 11788.

(37) Sillanp, A. J.; Laasonen, K. *Phys. Chem. Chem. Phys.* **2004**, *6*, 555.

(38) Cavallari, M.; Cavazzoni, C.; Ferrario, M. *Mol. Phys.* **2004**, *102*, 959.

(39) Ramaniah, L. M.; Bernasconi, M.; Parrinello, M. *J. Chem. Phys.* **1999**, *111*, 1587.

(40) Krekeler, C.; Hess, B.; Delle Site, L. *J. Chem. Phys.* **2006**, *125*, 054305.

(41) Izvekov, S.; Philpott, M. R. *J. Chem. Phys.* **2000**, *113*, 10676.

(42) (a) Raugei, S.; Klein, M. L. *J. Am. Chem. Soc.* **2001**, *123*, 9484. (b) Raugei, S.; Klein, M. L. *J. Chem. Phys.* **2002**, *116*, 196.

(43) Pagliai, M.; Cardini, G.; Schettino, V. *J. Phys. Chem. B* **2005**, *109*, 7475.

(44) Kirchner, B.; Seitsonen, A. P.; Hutter, J. *J. Phys. Chem. B* **2006**, *110*, 11475.

(45) Allen, P. G.; Bucher, J. J.; Shuh, D. K.; Edelstein, N. M.; Craig, I. *Inorg. Chem.* **2000**, *39*, 595.

(46) Petit, L.; Borel, A.; Daul, C.; Maldivi, P.; Adamo, C. *Inorg. Chem.* **2006**, *45*, 7382.

(47) Car, R.; Parrinello, M. *Phys. Rev. Lett.* **1985**, *55*, 2471.

(48) Loeffler, H. H.; Rode, B. M. *J. Chem. Phys.* **2002**, *117*, 110.

(49) *CPMD*, v.3.9; IBM Corp.: Armonk, NY, 1990−2004; MPI für Festkörperforschung: Stuttgart, Germany, 1997−2001.

(50) (a) Becke, A. D. *Phys. Rev. A: At., Mol., Opt. Phys.* **1988**, *38*, 3098. (b) Perdew, J. P. *Phys. Rev. B: Condens. Matter Mater. Phys.* **1986**, *33*, 8822.

(51) (a) Vetere, V.; Maldivi, P.; Adamo, C. *J. Comput. Chem.* **2003**, *24*, 850. (b) Vetere, V.; Maldivi, P.; Adamo, C. *Int. J. Quantum Chem.* **2003**, *91*, 321.

(52) Guillaumont, D. *J. Phys. Chem. A* **2004**, *108*, 6893.

(53) Sprik, M.; Hutter, J.; Parrinello, M. *J. Chem. Phys.* **1996**, *105*, 1142.

(54) Troullier, N.; Martins, J. L. *Phys. Rev. B: Condens. Matter Mater. Phys.* **1991**, *43*, 1993.

(55) Kleinman, L.; Bylander, D. M. *Phys. Rev. Lett.* **1982**, *48*, 1425.

(56) *Gaussian 03*, revision D.01; Frisch, M. J.; Trucks, G. W.; Schlegel, H. B.; Scuseria, G. E.; Robb, M. A.; Cheeseman, J. R.; Montgomery, J. A., Jr.; Vreven, T.; Kudin, K. N.; Burant, J. C.; Millam, J. M.; Iyengar, S. S.; Tomasi, J.; Barone, V.; Mennucci, B.; Cossi, M.; Scalmani, G.; Rega, N.; Petersson, G. A.; Nakatsuji, H.; Hada, M.; Ehara, M.; Toyota, K.; Fukuda, R.; Hasegawa, J.; Ishida, M.; Nakajima, T.; Honda, Y.; Kitao, O.; Nakai, H.; Klene, M.; Li, X.; Knox, J. E.; Hratchian, H. P.; Cross, J. B.; Bakken, V.; Adamo, C.; Jaramillo, J.; Gomperts, R.; Stratmann, R. E.; Yazyev, O.; Austin, A. J.; Cammi, R.; Pomelli, C.; Ochterski, J. W.; Ayala, P. Y.; Morokuma, K.; Voth, G. A.; Salvador, P.; Dannenberg, J. J.; Zakrzewski, V. G.; Dapprich, S.; Daniels, A. D.; Strain, M. C.; Farkas, O.; Malick, D. K.; Rabuck, A. D.; Raghavachari, K.; Foresman, J. B.; Ortiz, J. V.; Cui, Q.; Baboul, A. G.; Clifford, S.; Cioslowski, J.; Stefanov, B. B.; Liu, G.; Liashenko, A.; Piskorz, P.; Komaromi, I.; Martin, R. L.; Fox, D. J.; Keith, T.; Al-Laham, M. A.; Peng, C. Y.; Nanayakkara, A.; Challacombe, M.; Gill, P. M. W.; Johnson, B.; Chen, W.; Wong, M. W.; Gonzalez, C.; Pople, J. A. Gaussian, Inc.: Wallingford, CT, 2004.

(57) Refson, K. *Comput. Phys. Commun.* **2000**, *126*, 310.

(58) Dang, L. X. *J. Chem. Phys.* **1992**, *96*, 6970.

(59) Grossman, J. C.; Schwegler, E.; Draeger, E. W.; Gygi, F.; Galli, G. *J. Chem. Phys.* **2004**, *120*, 300.

(60) (a) Silvestrelli, P. L.; Marzari, N.; Vanderbilt, D.; Parrinello, M. *Solid State Commun.* **1998**, *107*, 7.

(61) (b) Marzari, N.; Vanderbilt, D. *Phys. Rev. B: Condens. Matter Mater. Phys.* **1997**, *56*, 12847. Humphrey, W.; Dalke, A.; Schulten, K. *J. Mol. Graphics* **1996**, *14*, 33.

(62) Gilli, P.; Bertolasi, V.; Ferretti, V.; Gilli, G. *J. Am. Chem. Soc.* **1994**, *116*, 909.

(63) Scheiner, S. *Hydrogen Bonding, A Theoretical Perspective*; Oxford University Press: New York, 1997.

(64) Ansell, S.; Neilson, G. W. *J. Chem. Phys.* **2000**, *112*, 3942.

(65) Neilson, G. W.; Enderby, J. E. *Proc. R. Soc. London, Ser. A* **1983**, *390*, 353.

(66) Clough, S. A.; Beers, Y.; Klein, G. P.; Rothman, L.S. *J. Chem. Phys.* **1973**, *59*, 2254.

(67) Silvestrelli, P. L.; Parrinello, M. *J. Chem. Phys.* **1999**, *111*, 3572.

(68) (a) Silvestrelli, P. L.; Parrinello, M. *Phys. Rev. Lett.* **1999**, *82*, 3308. (b) Silvestrelli, P. L.; Parrinello, M. *Phys. Rev. Lett.* **1999**, *82*, 5415.

(69) Badyal, Y. S.; Saboungi, M.-L.; Price, D. L.; Shastri, S. D.; Haeffner, D. R.; Soper, A. K. *J. Chem. Phys.* **2000**, *112*, 9206.

(70) Batista, E. R.; Xantheas, S. S.; Jonsson, H. *J. Chem. Phys.* **1998**, *109*, 4546.

(71) Laasonen, K.; Sprik, M.; Parrinello, M. *J. Chem. Phys.* **1993**, *99*, 9080.

(72) Coudert, F.-X.; Vuilleumier, R.; Boutin, A. *Chem. Phys. Chem.* **2006**, *7*, 2464.

(73) Hribar, B.; Southall, N. T.; Vlachy, V.; Dill, K. A. *J. Am. Chem. Soc.* **2002**, *124*, 12302.

(74) Ichikawa, K.; Kameda, Y.; Matsumoto, T.; Misawa, M. *J. Phys. C: Solid State Phys.* **1984**, *17*, L725.

(75) Nygard, K.; Hakala, M.; Manninen, S.; Hämäläinen, K.; Itou, M.; Andrejczuk, A.; Sakurai, Y. *Phys. Rev. B: Condens. Matter Mater. Phys.* **2006**, *73*, 024208.

(76) Soper, A. K.; Phillips, M. G. *Chem. Phys.* **1986**, *107*, 47.

(77) Thiessen, W. E.; Narten, A. H. *J. Chem. Phys.* **1982**, *77*, 2656.

(78) Soper, A. K. *J. Chem. Phys.* **1994**, *101*, 6888.

CT800007V